

# Structural Optimization and Vibration Control using Magneto-Rheological Dampers in Tall Buildings under Dynamic Wind Load

Alex Koch de Almeida<sup>1</sup>, Letícia Fleck Fadel Miguel<sup>2</sup>

<sup>1</sup>Postgraduate Program in Civil Engineering (PPGEC), Federal University of Rio Grande do Sul (UFRGS)  
Av. Osvaldo Aranha n°99, 90035-190, Porto Alegre, Rio Grande do Sul, Brazil.  
alex.almeida@ufrgs.br

<sup>2</sup>Department of Mechanical Engineering (DEMEC), Postgraduate Program in Mechanical Engineering (PROMECA), Postgraduate Program in Civil Engineering (PPGEC), Federal University of Rio Grande do Sul (UFRGS)  
Av. Sarmiento Leite n°425, 90050-170, Porto Alegre, Rio Grande do Sul, Brazil.  
letffm@ufrgs.br

**Abstract.** The importance of the wind action in structures, in a context in which the maximum possible and acceptable slenderness is desired, increases directly and proportionally to the height of the buildings. Those tall and slender buildings, respecting safety criteria, always aim at the minimum cost. This work is part of that scenario, which aimed to apply structural optimization methods combined with the use of Magneto-rheological (MR) dampers in tall buildings under dynamic wind load. The structure, idealized in concrete, was modeled using the finite element method and, the dynamic wind load, through a stochastic process. The optimization of the structure's mass was performed using the Particle Swarm Optimization (PSO) algorithm. Finally, a set of MR dampers (RD-1005-03, Lord Corporation), considering the modified Bouc-Wen rheological model with parameters obtained experimentally was applied in the structure. The results showed that the structural optimization combined with the control produced by the MR dampers was able to reduce the response, demonstrating that smart structures, which combine optimization techniques and semi-active control in their design, are a promising alternative.

**Keywords:** Tall buildings, wind load, structural optimization, Magneto-rheological damper.

## 1 Introduction

The state of the art in structural engineering is not even close to be reached. There are several variables and options representing a universe of possibilities that must be studied and developed. On one hand, we have slender structures that need to be safe and at the lowest possible cost, and here appears the dynamic loads, as the wind load, that must be supported, on another hand we have the tools to do that. In this paper we will travel through this universe, passing by two areas: structural optimization and vibration control using MR dampers. Several studies have emerged in the application and development of control strategies against dynamic forces, Dyke *et al* [1], Lee *et al* [2], Zhu *et al* [3], Ni *et al* [4], Carneiro [5], Askari *et al* [6], Kim and Kang [7], Bitaraf and Hurlebaus [8], César [9], Al-Fahdawi *et al* [10] and in the optimization area we can see recent publications about adjust, comparison and application, like Basílio *et al* [11], Souza and Miguel [12], Resende *et al* [13] and Weber *et al* [14]. In this work, these concepts will be addressed and applied.

## 2 Theoretical background

A building previously proposed and analyzed by Marcadella and Alberti [15] was taken as the object of this study. The building, designed in reinforced concrete, is symmetrical and has dimensions in the plan of 15m x 15m, 35 floors, 99.75m high, 2.85m high between slabs and 12cm thick on each slab. One of the building's frames was considered in this research, discretized into 144 nodes, 245 bars and 432 degrees of freedom. The 2D frame is

fixed in the base and horizontally requested by the action of the wind which was applied to the external nodes considering the areas of influence of the wind incidence of each one of them, as illustrated in Fig. 1.

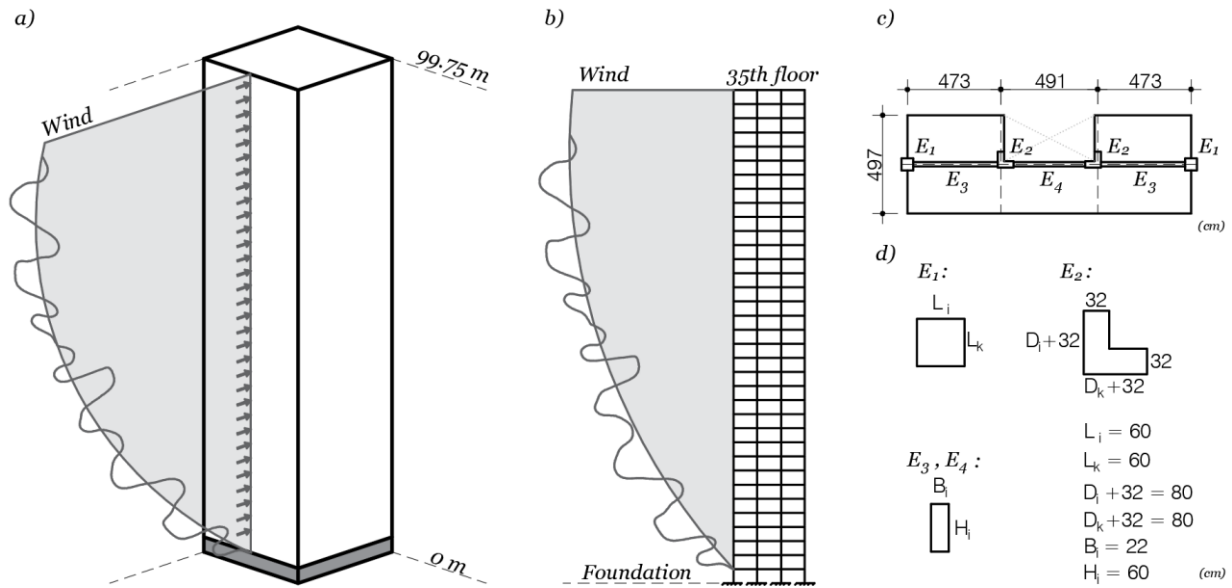


Figure 1. Analyzed structure. a) Perspective b) Theoretical 2D Frame c) Floor plan section considered d) Columns cross sections ( $E_1$  and  $E_2$ ) and beams cross section ( $E_3$  and  $E_4$ )

The problem was approached through the finite element method, according to the procedures of Clough and Penzien [16], Soriano [17] and Hibbeler [18]. The mass matrix of the structure was obtained by a combination of consistent and lumped mass matrices, considering the mass of the slabs. Once global mass and stiffness matrices,  $M$  and  $K$ , respectively, were carried out, then the damping matrix  $C$  was determined from the Rayleigh method.

About the wind load, its average component was obtained through the procedures described by ABNT NBR 6123 [19], and its fluctuating component through a stochastic process, as indicated by Shinozuka and Jan [20], Blessmann [21] and Miguel *et al.* [22], considering Davenport power spectra. The wind load on the top floor of the building over the analysis time is shown in Fig. 2, in which  $F_D$  is the Drag Force.

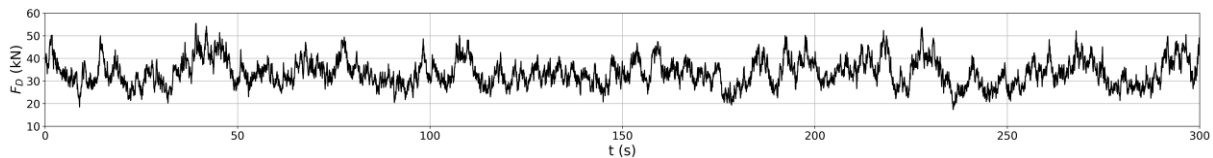


Figure 2. Drag Force on the top floor

### 3 Optimization of structure mass

A certain amount of mass was made available and optimally distributed in the elements of the structure. Since the dynamic wind excitation has a high spectral potential at low frequencies (less than 1Hz), the objective was to maximize the structure's first natural frequency ( $f_1$ ). The formal assembly of the problem is approached, according to Arora [23], through eq. (1):

$$\text{Minimize: } \frac{1}{f_1(i)}, \text{ Subject to: } g(i) \geq 0. \quad (1)$$

in which  $g(i)$  are the constraints imposed to the problem and  $i$  are the variables. For the studied problem, the restrictions imposed have their origin in the architecture and in the minimum resistance that each element needs. The loads and architecture considered for formulating the constraints were those elucidated by Marcadella and Alberti [15]. Furthermore, the symmetry of the structure was kept. The columns were grouped into external and

internal,  $E_1$  and  $E_2$  in Fig. 1, respectively. The beams were grouped into lateral and central,  $E_3$  and  $E_4$  in Fig. 1, respectively. And then, the elements of the same group were again grouped every 5 floors. Finally, a restriction of a constructive nature was imposed: Upper columns should have smaller dimensions than adjacent lower ones. The dimensions of the  $i$  variables, with  $i = \{1 \text{ to } 42\}$ , are shown in Fig. 1, in which the relation  $L_i = L_k$  and  $D_i = D_k$  was kept. The problem was solved using the widely studied Particle Swarm Optimization (PSO) algorithm, Kennedy and Eberhart [24], Shi and Eberhart [25], Engelbrecht [26]. Four parameters were provided to the algorithm:  $S_s$  is the number of particles in the swarm (taken equal 84),  $w$  is the inertia weight that controls the contribution of the previous velocity in the new velocity of the particle (taken equal 0.9),  $P_1$  and  $P_2$  are acceleration coefficients, that express how much confidence a particle has in itself or in its neighbors, respectively, those were taken variable (iteration 0 to 1000: 1.8 and 1.8, iteration 1000 to 1500: 2 and 1.6, iteration 1500 to 2000: 1.6 and 2, respectively). The bounds, constrictions and the optimal values for each group are shown in Tab. 1:

Table 1. Optimization problem summary

Group	Floor	Variable	Bounds (m)	g(i)	Optimal value (m)
G <sub>1</sub>	0 to 5	L <sub>1</sub>	0.60 to 1.20	L <sub>1</sub> - L <sub>3</sub> ≥ 0	1.20
G <sub>2</sub>	0 to 5	D <sub>2</sub>	0.48 to 1.83	D <sub>2</sub> - D <sub>4</sub> ≥ 0	1.18
G <sub>3</sub>	5 to 10	L <sub>3</sub>	0.55 to 1.20	L <sub>3</sub> - L <sub>5</sub> ≥ 0	1.15
G <sub>4</sub>	5 to 10	D <sub>4</sub>	0.43 to 1.83	D <sub>4</sub> - D <sub>6</sub> ≥ 0	1.13
G <sub>5</sub>	10 to 15	L <sub>5</sub>	0.50 to 1.20	L <sub>5</sub> - L <sub>7</sub> ≥ 0	1.00
G <sub>6</sub>	10 to 15	D <sub>6</sub>	0.33 to 1.83	D <sub>6</sub> - D <sub>8</sub> ≥ 0	1.08
G <sub>7</sub>	15 to 20	L <sub>7</sub>	0.45 to 1.20	L <sub>7</sub> - L <sub>9</sub> ≥ 0	0.85
G <sub>8</sub>	15 to 20	D <sub>8</sub>	0.23 to 1.83	D <sub>8</sub> - D <sub>10</sub> ≥ 0	1.03
G <sub>9</sub>	20 to 25	L <sub>9</sub>	0.40 to 1.20	L <sub>9</sub> - L <sub>11</sub> ≥ 0	0.55
G <sub>10</sub>	20 to 25	D <sub>10</sub>	0.13 to 1.83	D <sub>10</sub> - D <sub>12</sub> ≥ 0	0.73
G <sub>11</sub>	25 to 30	L <sub>11</sub>	0.30 to 1.20	L <sub>11</sub> - L <sub>13</sub> ≥ 0	0.45
G <sub>12</sub>	25 to 30	D <sub>12</sub>	0.03 to 1.83	D <sub>12</sub> - D <sub>14</sub> ≥ 0	0.58
G <sub>13</sub>	30 to 35	L <sub>13</sub>	0.20 to 1.20	-	0.25
G <sub>14</sub>	30 to 35	D <sub>14</sub>	0.03 to 1.83	-	0.48
G <sub>15</sub>	0 to 5	B <sub>15</sub> , H <sub>16</sub>	0.20 to 0.30, 0.50 to 0.70	-	0.30, 0.55
G <sub>16</sub>	0 to 5	B <sub>17</sub> , H <sub>18</sub>	0.20 to 0.30, 0.50 to 0.70	-	0.25, 0.70
G <sub>17</sub>	5 to 10	B <sub>19</sub> , H <sub>20</sub>	0.20 to 0.30, 0.50 to 0.70	-	0.30, 0.60
G <sub>18</sub>	5 to 10	B <sub>21</sub> , H <sub>22</sub>	0.20 to 0.30, 0.50 to 0.70	-	0.25, 0.70
G <sub>19</sub>	10 to 15	B <sub>23</sub> , H <sub>24</sub>	0.20 to 0.30, 0.50 to 0.70	-	0.30, 0.70
G <sub>20</sub>	10 to 15	B <sub>25</sub> , H <sub>26</sub>	0.20 to 0.30, 0.50 to 0.70	-	0.25, 0.70
G <sub>21</sub>	15 to 20	B <sub>27</sub> , H <sub>28</sub>	0.20 to 0.30, 0.50 to 0.70	-	0.30, 0.70
G <sub>22</sub>	15 to 20	B <sub>29</sub> , H <sub>30</sub>	0.20 to 0.30, 0.50 to 0.70	-	0.25, 0.65
G <sub>23</sub>	20 to 25	B <sub>31</sub> , H <sub>32</sub>	0.20 to 0.30, 0.50 to 0.70	-	0.25, 0.65
G <sub>24</sub>	20 to 25	B <sub>33</sub> , H <sub>34</sub>	0.20 to 0.30, 0.50 to 0.70	-	0.30, 0.65
G <sub>25</sub>	25 to 30	B <sub>35</sub> , H <sub>36</sub>	0.20 to 0.30, 0.50 to 0.70	-	0.20, 0.65
G <sub>26</sub>	25 to 30	B <sub>37</sub> , H <sub>38</sub>	0.20 to 0.30, 0.50 to 0.70	-	0.25, 0.65
G <sub>27</sub>	30 to 35	B <sub>39</sub> , H <sub>40</sub>	0.20 to 0.30, 0.50 to 0.70	-	0.25, 0.50
G <sub>28</sub>	30 to 35	B <sub>41</sub> , H <sub>42</sub>	0.20 to 0.30, 0.50 to 0.70	-	0.20, 0.55

The final value of the inverse of the objective function was  $f_1 = 0.5$  Hz. The evolution of the optimization process is shown in Fig. 3:

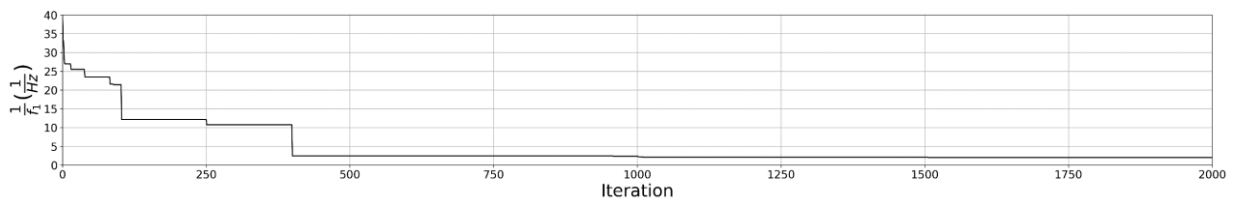


Figure 3. Cost history

## 4 Semi-active control using MR dampers

Semi-active dampers have mechanical properties or parameters that can be adjusted to improve their performance like an active control system while maintaining the reliability of passive control systems, Spencer Jr. *et al* [27]. These devices are basically composed of a magneto-rheological fluid that can change its properties in nanoseconds due to the presence of a magnetic field caused by a controllable current. Many rheological models were developed to numerically describe the hysteretic phenomenon inherent in these types of devices. In this study the modified Bouc-Wen model was used as shown in Fig. 4:

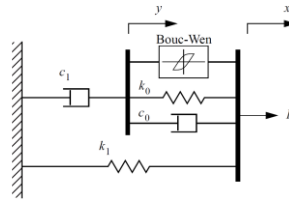


Figure 4. Modified Bouc-Wen model by Spencer Jr *et al* [27].

This model is described by eq. (2), eq. (3) and eq. (4), as follows:

$$F_{MR} = c_1 \dot{y} + k_1(x - x_0). \quad (2)$$

$$\dot{y} = \frac{1}{c_0 + c_1} [\alpha z + c_0 \dot{x} + k_0(x - y)]. \quad (3)$$

$$\dot{z} = -\gamma |\dot{x} - \dot{y}| |z|^{n_{bw}-1} - \beta (\dot{x} - \dot{y}) |z|^{n_{bw}} + A_{bw} (\dot{x} - \dot{y}). \quad (4)$$

in which  $F$  or  $F_{MR}(t)$ , is the total force generated by the system,  $c_0$  is the viscous damping observed at larger velocities,  $k_0$  is present to control the stiffness at large velocities,  $c_1$  is a dashpot included in the model to produce the roll-off observed at low velocities,  $k_1$  is the accumulator stiffness,  $x$  and  $y$  are the damper displacements,  $z$  is the evolutionary variable,  $x_0$  is the initial displacement of spring  $k_1$  associated with the nominal damper force due to the accumulator. The dot above a variable indicates time derivative.  $\alpha$ ,  $\beta$ ,  $\gamma$ ,  $A_{bw}$  and  $n_{bw}$  are parameters that describe the system hysteresis. Those parameters, shown in Tab. 2, were determined experimentally by César [9] for the RD-1005-3 MR damper (Lord corporation), which was used in this study; being  $I$  the current supplied to the equipment, whose maximum value is 0.5A.

Table 2. Modified Bouc-Wen model – Parameters of the RD-1005-3 MR damper, adapted from César [10]

Independent parameters	$A_{bw} [-]$	$\beta [\text{mm}^{-1}]$	$\gamma [\text{mm}^{-1}]$	$k_0 [\text{N}/\text{mm}]$	$k_1(x - x_0) [\text{N}]$	$n_{bw}$
	10.013	3.044	0.103	1.121	40	2
Current dependent parameters	$\alpha(I) = -826.67I^3 + 905.14I^2 + 412.52I + 38.24 [\text{N}]$ $c_0(I) = -11.73I^3 + 10.51I^2 + 11.02I + 0.59 [\text{N} \cdot \text{s}/\text{mm}]$ $c_1(I) = -54.40I^3 + 57.03I^2 + 64.57I + 4.73 [\text{N} \cdot \text{s}/\text{mm}]$					

Since RD-1005-3 MR damper is a low-capacity equipment, to simulate robust equipment compatible with the wind loads, 20 of these dampers acting in parallel were considered in each  $m$  controlled mass by a  $F_{MR}^m$  damper force, with  $m = \{1 \text{ to } 34\}$ . The  $F_{MR}^m$  damper forces were applied in the central frames of the structure, as shown in Fig. 5:

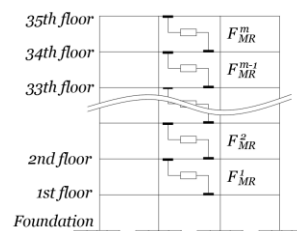


Figure 5. Dampers position

After applying the dampers, the dynamic equilibrium equation becomes, as eq. (5):

$$M\ddot{\vec{x}} + C\dot{\vec{x}} + K\vec{x} = \vec{F} - \vec{F}_{MR}. \quad (5)$$

in which  $\ddot{\vec{x}}$  is the acceleration vector,  $\dot{\vec{x}}$  is the velocity vector,  $\vec{x}$  the displacement vector and  $\vec{F}$  is the external force vector with the  $F_D$  at the indicated degrees of freedom and  $\vec{F}_{MR}$  is the damper force vector with the  $F_{MR}$  at the indicated degrees of freedom. To solve eq. (5) a numerical integration method can be applied.

To take advantage of the semi-active nature of the dampers, a Linear Quadratic Regulator was used, Meirovitch [28], Ogata [29], through the Clipped Optimal strategy (CO-LQR), Zhu *et al* [3], Ni *et al* [4], César [9], Carneiro [5]. The complete deduction of the theory can be appreciated in Carneiro [5], briefly the optimal control force at each instant of time can be determined by eqs. (6-8):

$$\vec{f}_o(t) = -\frac{1}{2}R^{-1}B^T P \vec{e}(t). \quad (6)$$

$$PA - \frac{1}{2}PBR^{-1}B^T + A^T P + 2Q = 0. \quad (7)$$

$$A = \begin{bmatrix} 0_{(n,n)} & Id_{(n,n)} \\ -M^{-1}K & -M^{-1}C \end{bmatrix}, B = \begin{bmatrix} 0_{(n,n)} \\ M^{-1}\Gamma_{(n,m)} \end{bmatrix}, \vec{e}(t) = \begin{bmatrix} x_n(t) \\ \dot{x}_n(t) \end{bmatrix}, Q = \begin{bmatrix} K & 0_{(n,n)} \\ 0_{(n,n)} & 0_{(n,n)} \end{bmatrix}, R = 10^{-7}Id_{(m,m)} \quad (8)$$

in which  $\vec{f}_o(t)$  is the optimal force vector at each instant of time, with  $m$  optimal forces  $f_o$ ,  $\vec{e}(t)$  is the state vector of the system which is composed by the  $n$  displacement  $x(t)$  and  $n$  velocities  $\dot{x}(t)$ , where  $n$  is the number of degrees of freedom,  $B$  is the matrix that describes the control forces in the state space representation,  $\Gamma$  is a matrix describing the location of the  $m$  control forces.  $Q$  and  $R$  are called weighting matrices, high values for elements of  $Q$  means prioritizing response reduction over control forces, high values for elements of  $R$  means the opposite, in general those values are obtained by testing the best response, in this study were used those indicated by Carneiro [5].  $A$  is the state matrix of the system and  $Id$  is the identity matrix. Eq. (7) is the reduced Riccati equation, and  $P$  is the Riccati matrix.

Once  $\vec{f}_o(t)$  has been determined, the selection of the current applied to the damper can be obtained through the eq. (9):

$$I = I_{max}H[(f_o - F_{MR})F_{MR}]. \quad (9)$$

in which  $I_{max}$  is the maximum current, associated with the magnetic field saturation and  $H(-)$  is the Heaviside function. This way, the force of the damper is indirectly controlled, through the control of the current, that is, when the damper is providing the optimum force, the applied current remains unchanged, if the magnitude of the force produced by the damper is less than the magnitude of the optimal desired force and the two forces have the same sign, the applied current is increased to the maximum level.

## 5 Results and Discussions

The analysis was based on observing the response to wind load over the time (300 s) in three configurations: the original structure presented in chapter two (Original Uncontrolled, or S1), the optimal structure obtained in chapter three (Optimal Uncontrolled, or S2) and the optimal structure with 34 MR dampers following the procedure presented in chapter four (Optimal 34MR CO-LQR, or S3). The maximum response of the three configurations at each floor is shown in Fig. 6, and the response over time on the top floor is shown in Fig. 7:

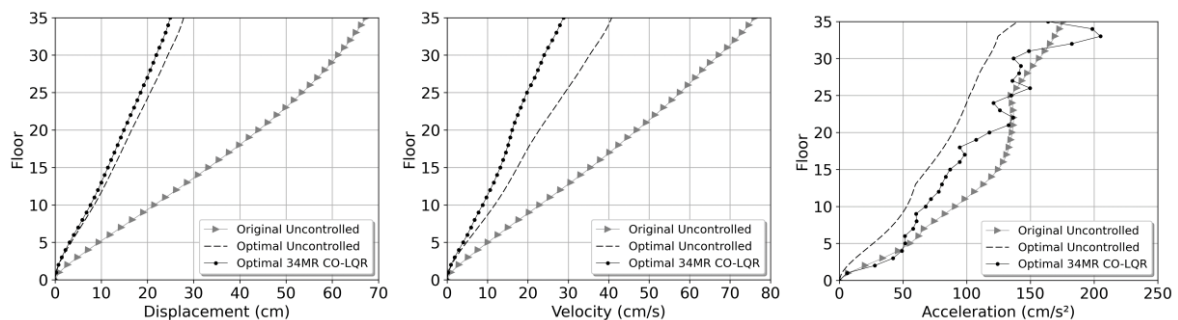


Figure 6. Maximum response

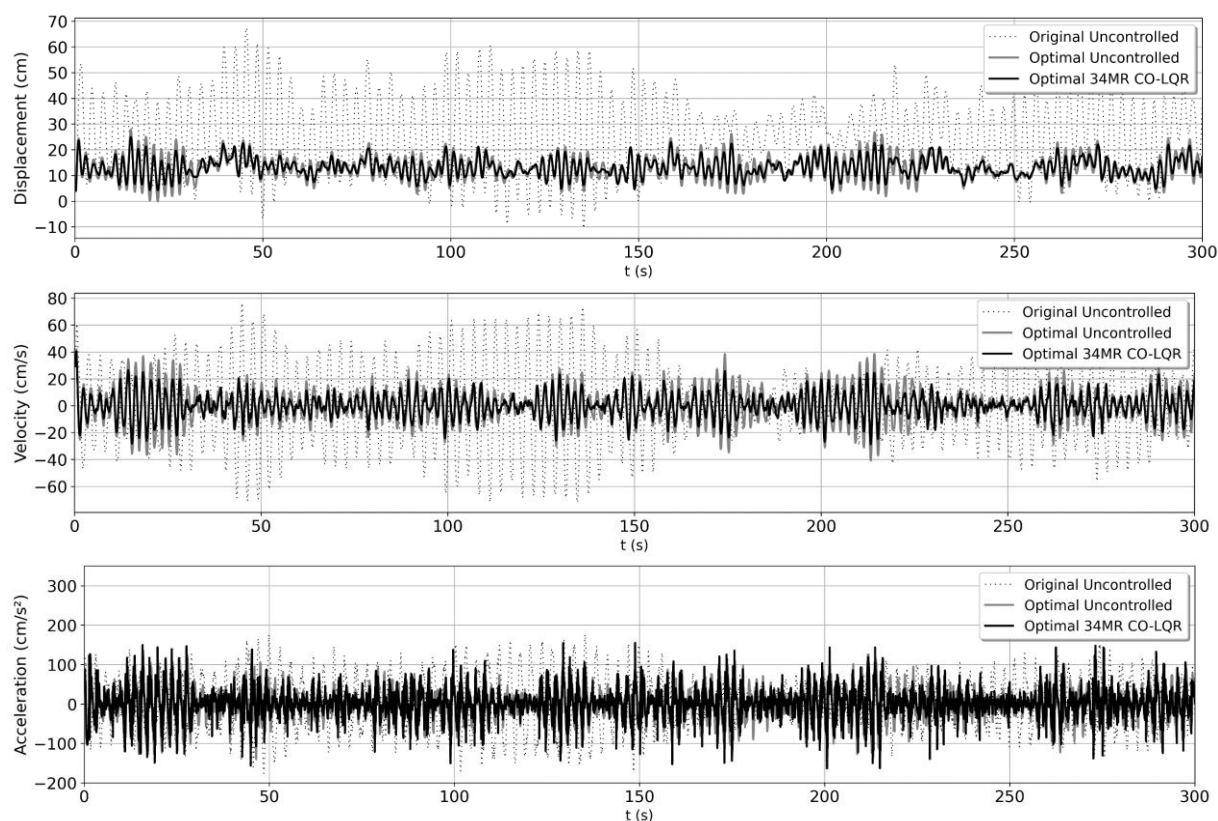


Figure 7. Response over time on the top floor

The maximum displacements on the top floor were 67.4 cm, 27.9 cm, 24.9 cm, from S1, S2 and S3 configurations, respectively. S2 and S3 showed a reduction of 58.6% and 63.1%, respectively, compared to S1, and S3 showed a reduction of 10.75% compared to S2. The results also showed that the maximum story drift between two consecutive floors were 2.4 cm, 1 cm, 0.9 cm, from S1, S2 and S3 configurations, respectively. It is possible to observe that the displacements over time were controlled.

The maximum velocities on the top floor are 76.2 cm/s, 40.7 cm/s, 28.8 cm/s, from S1, S2 and S3 configurations, respectively. S2 and S3 showed a reduction of 46.5% and 62.2%, respectively, compared to S1, and S3 showed a reduction of 29.3% compared to S2. It is possible to observe that the velocities over time were controlled.

The maximum accelerations on the top floor are 176.3 cm/s<sup>2</sup>, 140.2 cm/s<sup>2</sup>, 162.3 cm/s<sup>2</sup>, from S1, S2 S3 configurations, respectively. S2 and S3 showed a reduction of 20.5% and 7.9%, respectively, compared to S1, and S3 showed an increase of 15.8% compared to S2. Moreover, we can see an acceleration peak of 209 cm/s<sup>2</sup>, between the 30<sup>th</sup> and 35<sup>th</sup> floors. In terms of percent gravity acceleration (g%), the maximum values were 18g%, 14.3g%, 21.3g%, from S1, S2 and S3 configurations, respectively. It is possible to observe that the accelerations showed a reduction most of the time, however smaller than displacements and velocities, and demonstrating some peaks over the time.

## 6 Conclusions

The results showed a considerable reduction in the response of the structure. Most of the reduction was due to the optimization of the mass demonstrated in chapter three, however a part of the reduction percentage was due to the work of the MR dampers applied according to chapter four, which prove to be another tool in the control of vibrations. It should be noted that there is a potential to be explored in the use of MR dampers, such as: position optimization, maximum force optimization and calibration of LQR control parameters, that is, the contribution in response control can be optimized. In this sense, advances in research are of great importance, and smart structures, which combine optimization techniques and semi-active control in their design, are a promising alternative, which must be studied and developed.

**Acknowledgments.** The authors acknowledge the financial support of CAPES and CNPq.

**Authorship statement.** The authors hereby confirm that they are the sole liable persons responsible for the authorship of this work, and that all material that has been herein included as part of the present paper is either the property (and authorship) of the authors, or has the permission of the owners to be included here.

## References

- [1] S. J. Dyke, B. F. Spencer Jr., M. K. Sain, J. D. Carlson, “An Experimental Study of MR Dampers for Seismic Protection”. *Smart Materials and Structures: Special Issue on Large Civil Structures*, 1999.
- [2] J. H. K. Lee, R. K. L. Su, P. K. K. Lee, L. C. H. Lam, “Semi-Active Damping Device For Vibration Control Of Buildings Using Magnetorheological Fluid”. *Advances in Building Technology*, vol. 2, pp. 969–976, 2002.
- [3] W. Q. Zhu, M. Luo, L. Dong, “Semi-active control of wind excited building structures using MR/ER dampers”. *Probabilistic Engineering Mechanics* 19, pp. 279–285, 2004.
- [4] Y. Q. Ni, Z.G. Yingb, J.Y. Wanga, J.M. Koa, B.F. Spencer Jr.c, “Stochastic optimal control of wind-excited tall buildings using semi-active MR-TLCDs”. *Probabilistic Engineering Mechanics* 19, pp. 269–277, 2004.
- [5] R. B. Carneiro, “Controle Semi-Ativo De Vibrações Em Estruturas Utilizando Amortecedor Magnetorreológico”. PhD Thesis, Universidade de Brasília, 2009.
- [6] M. Askari, J. Li, B. Samali, “Semi-Active LQG Control of Seismically Excited Nonlinear Buildings using Optimal Takagi-Sugeno Inverse Model of MR Dampers”. *Procedia Engineering* 14, pp. 2765–2772, 2011.
- [7] H. Kim, J. Kang, “Semi-active fuzzy control of a wind-excited tall building using multi-objective genetic algorithm”. *Engineering Structures* 41, pp. 242–257, 2012.
- [8] M. Bitaraf, S. Hurlebaus, “Semi-active adaptive control of seismically excited 20-story nonlinear building”. *Engineering Structures* 56, pp. 2107–2118, 2013.
- [9] M. T. B César, “Vibration Control of Building Structures using MagnetoRheological Dampers”. PhD Thesis, FEUP, 2015.
- [10] O. A. S. Al-Fahdawi, L. R. Barroso, R.W. Soares, “Semi-active adaptive control for enhancing the seismic performance of nonlinear coupled buildings with smooth hysteretic behavior”. *Engineering Structures* 191, pp. 536–548, 2019.
- [11] S. C. A. Basílio, A. C. C. Lemonge, E. C. R. Carvalho, P. H. Hallak, “A Dynamic Treatment Criterion of Population Sizes in PSO”. *Proceedings of the XLI Ibero-Latin-American Congress on Computational Methods in Engineering*, 2020.
- [12] O. A. P. de Souza and L. F. F. Miguel, “Comparison of the performance of different metaheuristic optimization algorithms”. *Proceedings of the XLI Ibero-Latin-American Congress on Computational Methods in Engineering*, 2020.
- [13] C. H. B. Resende, A. C. C. Lemonge, P. H. Hallak, J. P.G. Carvalho, J. C. Motta, “Global stability and natural frequencies of vibration in multi-objective optimization of 3D steel frames”. *Proceedings of the XLI Ibero-Latin-American Congress on Computational Methods in Engineering*, 2020.
- [14] G. A. Weber, A. P. C. Quispe, R. Q. Rodríguez, “Structural Optimization of Reinforced Concrete Beams using GA method”. *Proceedings of the XLI Ibero-Latin-American Congress on Computational Methods in Engineering*, 2020.
- [15] C. Marcadella and F. A. Alberti, “Comparative analysis of horizontal displacements of three structural bracing systems subjected to static wind loads influence”. *Proceedings of the 59th Brazilian Concrete Congress*, 2017.
- [16] R. W. Clough and J. Penzien. *Dynamics of Structures*. Computers & Structures, Inc., 1995.
- [17] H. L. Soriano. *Elementos Finitos – Formulação e Aplicação na Estática e Dinâmica das Estruturas*. Editora Ciência Moderna Ltda., 2009.
- [18] R. C. Hibbeler. *Análise das estruturas*. Pearson Education do Brasil, 2013.
- [19] Associação Brasileira de Normas Técnicas. *NBR 6123: Forças devidas ao vento em edificações*. 1988.
- [20] M. Shinozuka, C. M. Jan. “Digital simulation of random processes and its applications”. *Journal of sound and vibration*, vol. 25, Issue 1, 1972.
- [21] Blessmann, J. *O vento na Engenharia Estrutural*. Editora da UFRGS, 1995.
- [22] L. F. F. Miguel, L. F. F. Miguel, J. D. Riera, J. Kaminski Jr., R. C. R. Menezes. “Assessment of code recommendations through simulation of EPS wind loads along a segment of a transmission line”. *Engineering Structures*, vol. 43, pp. 1-11, 2012.
- [23] J. S Arora. *Introduction to Optimum Design – Fourth Edition*. Elsevier, 2017.
- [24] J. Kennedy and R.C. Eberhart, “Particle Swarm Optimization”. *Proceedings of the IEEE International Joint Conference on Neural Networks*, pp. 1942-1948, 1995.
- [25] Y. Shi and R.C. Eberhart, “A modified particle swarm optimizer”. *Proceedings of the IEEE International Conference on Evolutionary Computation*, pp. 69-73, 1998.
- [26] A. P. Engelbrecht. “*An Introduction to Computational Intelligence*”. John Wiley & Sons, 2007.
- [27] B. F. Spencer Jr., S. J. Dyke, M. K. Sain, J. D. Carlson, “Phenomenological Model of a Magnetorheological Damper”. *ASCE Journal of Engineering Mechanics*, 1997.
- [28] L. Meirovitch. *Dynamics and control of structures*. John Wiley & Sons, 1990.
- [29] K. Ogata. *Modern Control Engineering*. Pearson Education, 2010.